

## Approximate Multiconfigurational Treatment of Spin-Coupled Metal Complexes

Guilherme Menegon Arantes\*<sup>†</sup> and Peter R. Taylor<sup>‡</sup>

*Instituto de Química, Universidade de São Paulo, Av. Lineu Prestes 748, 05508-900, São Paulo, SP, Brazil and Department of Chemistry, University of Warwick, Coventry, CV4 7AL, United Kingdom*

Received March 8, 2010

**Abstract:** The weak interaction between unpaired electrons in polynuclear transition-metal complexes is often described by exchange and spin polarization mechanisms. The resulting intrinsic multiconfigurational electronic structure for such complexes may be calculated with wave function-based methods (e.g., complete active space configuration interaction and complete active space self-consistent field), but computations become extremely demanding and even unfeasible for polynuclear complexes with a large number of open-shells. Here, several levels of selection of configurations and symmetry considerations that still capture the essential physics of exchange and spin polarization mechanisms are presented. The proposed approximations result in significantly smaller configuration interaction expansions and are equally valid for ab initio and semiempirical methods. Tests are performed in simple molecular systems and in small transition-metal complexes that cover a range of valence and charge states. In particular, superexchange contributions can be calculated to good accuracy using only single ionic excitations. Further reduction in the size of the configuration expansions is possible but restricts the description to low-lying spin ladders. The proposed configuration interaction schemes may be used to resolve space and spin symmetries in the calculation of electronic structures, exchange coupling constants, and other properties pertinent to polynuclear transition-metal complexes.

### 1. Introduction

Polynuclear transition-metal (TM) compounds with weakly coupled open-shell electrons have interesting magnetic properties as a consequence of the population at thermal energies of low-lying excited states with different total spins. The underlying interactions are traditionally mapped to a spin–spin coupling between momenta  $\mathbf{S}$  localized in neighboring magnetic sites and are often described by the Heisenberg–Dirac–van Vleck spin Hamiltonian:<sup>1</sup>

$$\hat{H}_{\text{HDvV}} = - \sum_{A < B} J_{AB} \mathbf{S}_A \cdot \mathbf{S}_B \quad (1)$$

where  $J_{AB}$  is the isotropic Heisenberg coupling constant between spins on sites A and B. Since  $[\hat{H}_{\text{HDvV}}, \hat{S}^2] = 0$ , the two operators share a common set of eigenstates. The eigenvalues correspond to a spin ladder, and the energy gaps between low-lying spin states depend linearly on the  $J$  coupling constant. For the simplest case of a pair of magnetic sites with spins  $\mathbf{S}_A$  and  $\mathbf{S}_B$ , the coupling is ferromagnetic, and  $J > 0$  in the sign convention assumed on eq 1, if the ground state is high-spin  $S = S_A + S_B$ . The coupling is antiferromagnetic, and  $J < 0$ , if the ground state is low-spin  $S = |S_A - S_B|$ . The spin–spin interaction modeled by eq 1 is in fact an effective one. As proposed by Heisenberg<sup>2</sup> and Dirac,<sup>3</sup> the interactions arise due to spin-independent Coulomb electron–electron repulsion and exchange symmetry.

First-principles calculations with the spin-free electronic Hamiltonian should then be able to predict spin eigenstates and  $J$  constants for TM compounds. Anderson<sup>4,5</sup> was seminal

\* Corresponding author. Email: garantes@iq.usp.br.

<sup>†</sup> Universidade de São Paulo.

<sup>‡</sup> University of Warwick.

in realizing how to extract the main contributions to the effective spin coupling from the electronic structure. His model can be understood by considering the following simple valence-bond (VB) scheme: A pair of magnetic sites A and B contain two weakly interacting electrons occupying two orthogonal orbitals (constructed by a suitable rotation of the molecular orbitals) labeled  $a$  and  $b$  localized on centers A and B, respectively. By weakly interacting it should mean that the two electrons do not form a covalent bond. This situation corresponds to a dihydrogen molecule at stretched bond distance or a spin-coupled Cu(II,  $d^9$ ) dimer. Four Slater determinants with  $M_S = 0$  can be constructed:  $|a\bar{b}|$ ,  $|\bar{a}b|$ ,  $|a\bar{a}|$ , and  $|\bar{b}\bar{b}|$ . The first two are “neutral” configurations, and the last two are charge-transfer “ionic” configurations. Their combination results in the following configuration state functions:

$$\begin{aligned} |^1\Psi_{\text{neu}}\rangle &= 2^{-1/2}[|a\bar{b}| - |\bar{a}b|] \\ |^1\Psi_{\text{ion}}^A\rangle &= |a\bar{a}| \\ |^1\Psi_{\text{ion}}^B\rangle &= |b\bar{b}| \\ |^3\Psi_{\text{neu}}\rangle &= 2^{-1/2}[|a\bar{b}| + |\bar{a}b|] \end{aligned} \quad (2)$$

The energy difference between the triplet  $|^3\Psi_{\text{neu}}\rangle$  and the singlet  $|^1\Psi_{\text{neu}}\rangle$  will be proportional to  $K_{ab}$ , the exchange integral between orbitals  $a$  and  $b$ .<sup>6</sup> This direct exchange interaction is ferromagnetic because the high-spin state (triplet) is favored. Configuration mixing between neutral and ionic states will lower the singlet energy and lead to the ground state:<sup>6</sup>

$$|^1\Psi_{\text{CI}}\rangle = (1 - \alpha)^{1/2}|^1\Psi_{\text{neu}}\rangle + \alpha^{1/2}|^1\Psi_{\text{ion}}\rangle \quad (3)$$

where  $|^1\Psi_{\text{ion}}\rangle$  is a superposition of the two ionic configuration state functions shown above and  $\alpha$  gives the degree of mixing between the neutral and ionic states. This mixing is equivalent to a virtual hopping of the electron from one magnetic site to the other (the charge-transfer ionic configurations), and it gives an antiferromagnetic contribution to spin-coupling because the low spin (singlet) is favored. In general, for weakly coupled open-shell compounds with several unpaired electrons, neutral configurations will appear in the wave function expansion for all spin states. Their contribution to spin coupling is ferromagnetic, i.e., stabilize the high-spin state, and is known as the *direct exchange* effect or mechanism. Ionic configurations will appear in expansions of all but the highest spin state and give antiferromagnetic contributions known as the through-space *superexchange* mechanism.

This simple VB model can be expanded to explicitly include an occupied valence closed shell of diamagnetic ligand bridges that coordinate metal ions in TM complexes. Ligand-to-metal charge-transfer (LMCT) excitations built out of a set of neutral and ionic configurations, equivalent to those on eq 3, will have either anti- or ferromagnetic contributions to spin coupling. This issue is discussed in more detail below. To make a connection with the jargon of previous perturbative treatments,<sup>7–9</sup> it should be noted that single LMCT excitations out of neutral configurations are usually called ligand spin polarization (LSP) because an

effective spin density appears on the bridge.<sup>8</sup> Double LMCT excitations are termed dynamic or double spin polarization (DSP). Excitations from core orbitals or to unoccupied orbitals have been suggested to account for dynamic correlation and orbital relaxation effects<sup>9,10</sup> and, hence, do not comprise additional spin-coupling mechanisms.

Another modification of the two electrons in two localized orbitals scheme presented above is the addition of a third electron resulting in a mixed valence compound such as the stretched  $\text{H}_2^-$  molecule. Delocalization or “resonance” of the excess electron between the magnetic sites A and B stabilizes the system and occurs favorably when the local spins  $\mathbf{S}_A$  and  $\mathbf{S}_B$  are aligned in parallel. This *double exchange* effect may then give effective ferromagnetic contributions to the spin coupling in mixed valence TM complexes.<sup>11,12</sup>

The method most widely used today to predict  $J$  coupling constants for polynuclear complexes is the broken-symmetry approach proposed by Noodleman.<sup>13,12</sup> In this single configuration description, the solution for the low-spin state (the BS state, corresponding to  $M_S = |S_A - S_B|$  in the above example with two magnetic centers) has space and spin symmetries broken. Such state is not a spin eigenstate but a superposition of spin states weighted by Clebsch–Gordan coefficients. A value for  $J$  can be estimated<sup>14</sup> by using spin-projection techniques and by also computing the highest spin (HS) state, which usually is well described by a single configuration:

$$J = -\frac{E_{\text{HS}} - E_{\text{BS}}}{\langle \hat{S}^2 \rangle_{\text{HS}} - \langle \hat{S}^2 \rangle_{\text{BS}}} \quad (4)$$

where  $E$  is the state energy and  $\langle \hat{S}^2 \rangle$  is the expectation value of the total spin operator. The success of the broken-symmetry approach can be traced to appropriate descriptions of direct exchange, superexchange, and LSP mechanisms discussed above.<sup>8</sup> However, its accuracy obviously depends on the electronic structure method employed for the single configuration calculations, which is often spin-polarized density functional theory. Because eigenfunctions for the lower spin states are not obtained explicitly, the broken-symmetry approach is not suited to study state specific properties. Nevertheless, mapping and spin-projection techniques may also be applied to estimate  $\mathbf{g}$  tensors and hyperfine coupling constants<sup>15</sup> and to optimize geometries<sup>16</sup> approximately. Along the same line, an extended broken-symmetry approach has been introduced recently that allows the calculation of energy derivatives for homovalent binuclear complexes.<sup>17</sup>

From the VB discussion in the previous paragraphs, it seems evident to employ configuration interaction (CI) of Slater determinants to compute wave functions for low-spin eigenstates. All spin-coupling mechanisms and electronic effects cited above can be naturally accounted for if an appropriate configuration space is used. However, the exponential scaling of the size of the CI space puts serious limitations on the range of TM complexes and properties that can be calculated with CI. For instance, the configurational space generated in full excitation level for about 18 unpaired electrons already exceeds the capacity of modern

CI code implementations and computer hardware. At this point, some heroic CI computations on low-spin states of binuclear TM complexes by Malrieu and collaborators should be mentioned.<sup>18,9</sup> Their dedicated difference CI method has been used to compute energy differences between spin multiplets in very good agreement with experimental data. Together with perturbative analysis, this CI method has also been used to identify contributions to spin coupling.<sup>9,10</sup> Even so, the dedicated difference CI also suffers from an exponential scaling of the CI space and thus is limited to binuclear complexes with a small number of unpaired electrons.

In this paper approximate levels of CI selection are proposed in trying to find short CI expansions that still capture the essential physics of spin coupling for the low-spin eigenstates. Determinants are built with localized molecular orbitals. But instead of specifying a given level of excitation from a single reference as in canonical CI, the configurational space is built by completing the spin manifold for neutral (or covalent), ionic, and ligand-to-metal charge-transfer VB-like structures. It is important to note that all approximations proposed here concern only the selection of configurations that enter in the CI. Thus, all the conclusions obtained should be equally valid irrespective of the method, semiempirical or *ab initio*, used to calculate the molecular integrals and configuration energies. A semiempirical Hamiltonian was employed here because future applications of the proposed approximations will use a hybrid quantum/classical potential based on semiempirical methods. Tests are performed in several simple systems so that full CI calculations can be carried out as references. Details of the computational methods are given in the next section. The results show that single ionic excitations between magnetic sites are enough to obtain an accurate superexchange contribution. Further reduction in the size of the CI space is possible but restricts the description to ground spin ladders. For iron–sulfur clusters, spin coupling can be correctly described by rather small CI expansions, paving the way for simulation studies of magnetic and electronic properties of these prosthetic groups in the condensed phase.

## 2. Computational Methods

Test calculations were performed on simple spin-coupled molecular systems. Two homonuclear diatomics,  $N_2$  and  $Cr_2$ , two bridged triatomics,  $N_2F^-$  and  $Fe_2S^{4+}$ , and the ring cluster  $Fe_2S_2^{2+}$ , were studied. Dinitrogen bond distance was set to 4.5 bohr ( $\sim 2.86$  Å), and the dichromium bond distance was set to 4.4 bohr ( $\sim 2.33$  Å). At such separations, covalent bonding is not significant, and energy splittings between the total spin eigenstates have magnitudes similar to those observed in polynuclear TM complexes. The equilibrium bond lengths for dinitrogen and dichromium are  $\sim 1.11$  and  $\sim 1.68$  Å, respectively. Each atom in the stretched diatomic molecule plays the role of an open-shell metal center or magnetic site. The unpaired electrons are weakly interacting, in a suitable model to the direct exchange and through-space superexchange mechanisms. Yet, dinitrogen is simple enough to allow complete expansions of the electronic wave function as well as several levels of CI selection. Neutral, dipositive, and mononegative total molecular charges were assigned for

dinitrogen as models of magnetic compounds with half-full open shell, less than half-full, and mixed valence, respectively. Triatomic molecules composed of two magnetic centers separated by a diamagnetic ligand are the simplest systems to probe the effect of the proposed approximations on interactions via the ligand spin polarization mechanism. Since bridge ligands found in TM complexes are usually diamagnetic anions, stretched dinitrogen was bridged with fluoride in an angular geometry with  $C_{2v}$  symmetry,  $\angle = 75^\circ$ ,  $d(N-F) = 1.80$  Å, and  $d(N-N) = 2.19$  Å. In the TM compound  $Fe_2S^{4+}$ , two Fe(III) are bridged by a sulfide ligand. A symmetric linear geometry was adopted with  $d(Fe-S) = 1.271$  Å. The binuclear iron–sulfur cluster  $Fe_2S_2^{1+/2}$  is the prosthetic group found in many electron-transfer proteins, such as ferredoxin. Each iron is also attached to the protein by two cysteine sulfur atoms, with a total tetrahedral coordination. By contrast, the bare  $Fe_2S_2^{2+}$  cluster studied here, a  $D_{2h}$  geometry was used,<sup>19</sup> with  $d(Fe-Fe) = 2.543$  and  $d(Fe-S) = 2.251$  Å. The  $z$  axis contains the two magnetic sites in all molecules studied.

Calculations were carried out with a semiempirical neglect of diatomic differential overlap (NDDO) Hamiltonian.<sup>20,21</sup> A slightly modified version of the MOPAC2000<sup>22,23</sup> code that allowed CI calculations using localized molecular orbitals was employed. Standard AM1 parameters were used for nitrogen and fluoride<sup>24</sup> and modified neglect of differential overlap (MNDO)-d parameters were used for sulfur.<sup>25</sup> MNDO-d parameters were not available for chromium and iron, so a quick parametrization had to be done. See details and the parameter values in the Supporting Information. Molecular orbitals (MOs) were obtained from high-spin restricted open-shell Hartree–Fock (ROHF) calculations and were localized using an equivalent Pipek–Mezey procedure.<sup>26</sup> Although MOPAC does not work with symmetry-adapted basis, all resulting wave functions were checked for the correct space and spin symmetries. Active spaces defined for the CASCI (full CI on the given active space)<sup>27</sup> calculations contained all open-shell MOs as well as outer valence unoccupied and double-occupied MOs in  $N_2^{+2}$  and  $N_2^-$ , respectively. All unpaired electrons were included in the active spaces. Full details of the active spaces used are given for each tested molecule in the Results and Discussion Section. Approximate CI expansions were based on the VB arguments presented in the Introduction. Hence, instead of specifying a given level of excitation from the ROHF solution, the selected CI expansions included all determinants needed to complete the spin manifold for a given level of approximation for the mechanisms of effective spin-coupling discussed. Only  $M_S = 0$  (or  $M_S = 0.5$ , for  $N_2^-$ ) determinants were used in the selected CI expansions.

For the larger active spaces, CASCI calculations were not feasible for the low-spin states (singlet and triplet). MOPAC generates and diagonalizes the CI matrix (or secular determinant) explicitly, and the code could not be compiled to use more than 2 GB of memory. Thus, the size of the CI expansions were limited to about 9000 configurations, which is less than the number of configurations necessary to expand the singlet and triplet states for the molecules formed by Cr and Fe. All the CASCI calculations were done with the

**Table 1.** Relative Energies (eV) and Number of Configurations (size) Included in the Wavefunction Expansions for Electronic Eigenstates of Dinitrogen in Neutral, Dipositive, and Negative Total Molecular Charge

		$N_2^0$			
CI expansion	size	$^1\Sigma_g$	$^3\Sigma_u$	$^5\Sigma_g$	$^7\Sigma_u$
CASCI	400	0.0000	0.0281	0.0876	0.1872
neu + single ion	80	0.0000	0.0278	0.0868	0.1864
neu + $p_x, p_y, p_z$ ion	56	0.0000	0.0278	0.0868	0.1864
neu + $p_z$ ion	32	0.0000	0.0262	0.0822	0.1778
neu + $p_x, p_y$ ion	44	0.0000	0.0014	0.0043	0.0087
		$N_2^{2+}$			
CI expansion	size	$^1\Sigma_u$	$^3\Sigma_g$	$^5\Sigma_u$	
CASCI	225	0.0000	0.0515	0.1953	
neu + single ion	162	0.0000	0.0514	0.1939	
neu + unpair, $p_z$ ion	114	0.0000	0.0514	0.1939	
neu $p_z$ + unpair, $p_z$ ion	72	0.0000	0.0514	0.1939	
neu + $p_z$ ion	78	0.0000	0.0567	0.2028	
neu + unpair ion	90	0.0000	-0.0029	-0.0087	
		$N_2^-$			
CI expansion	size	$^2\Sigma_u$	$^4\Sigma_g$	$^6\Sigma_u$	
CASCI	300	0.3125	0.1458	0.0000	
neu + single ion	240	0.3126	0.1458	0.0000	
neu $p_z$ + $p_z$ ion	44	0.3130	0.1460	0.0000	
neu	60	0.3298	0.1568	0.0000	
neu $p_z$	20	0.3298	0.1568	0.0000	

semiempirical NDDO Hamiltonian. The CASSCF method<sup>27</sup> within the MOLCAS 6.2 program system<sup>28</sup> was used to compute a reference value for the  $Fe_2S_2^{2+}$  cluster. This calculation was conducted with basis symmetry adapted to the  $D_{2h}$  point group, using the ANO-RCC<sup>29</sup> set with quadruple- $\zeta$  contraction (e.g., 7s6p4d3f2g for iron).

### 3. Results and Discussion

Results of several approximate levels of CI selection on the electronic structure of simple molecules are presented in this section. For the diatomic systems and the linear  $Fe_2S^{4+}$ , all spin ladders shown are  $\Sigma$  states. For  $NFN^-$ , the lowest energy spin states are alternating  $A_1$  and  $B_2$  states, and for the ring  $Fe_2S_2$ , the spin ladder shown has alternating  $A_g$  and  $B_{1u}$  states. For example, the correct energy ordering for the total spin eigenstates of neutral  $N_2$  is  $^1\Sigma < ^3\Sigma < ^5\Sigma < ^7\Sigma$ .

**3.1. Neutral  $N_2$ .** For neutral  $N_2$ , the following configuration is obtained after localizing the high-spin ROHF MOs:  $[(core)2s^A 2s^A 2s^B 2s^B 2p_z^A 2p_z^B 2p_x^A 2p_x^B 2p_y^A 2p_y^B]$ , where the over bar assigns spin down and the superscripts A and B are used to label each nitrogen atom. Localized MOs have large contributions by only one atomic function which is then used as a label. The six unpaired electrons in the six 2p MOs are responsible for the spin coupling and form the active space for generation of configurations used in the wave function expansion. Because of localization, the MOs will have a  $C_{\infty v}$  symmetry, which is lower than the nuclear point group.

The relative energies obtained for the lowest energy spin eigenstates are shown in Table 1. The CASCI has a total of 400 configurations with  $M_S = 0$ . There are 20 unpaired neutral configurations, i.e., with 1 electron in each of the 6

active MO. The septet wave function is composed only by these 20 configurations, with equal CI weights. The largest CI weights ( $\sim 0.24$  in the singlet state) in the expansions for all other spin states come from two configurations,  $|p_z^A p_z^B p_x^A p_x^B p_y^A p_y^B|$  (only the active space is represented on this and the following determinant configurations) and the respective A to B spin inversion. These two configurations correspond to a  $^4S$  high-spin state on each N atom. The second largest contributions come from the other 18 unpaired neutral configurations, such as  $|p_z^A p_z^B p_x^A p_x^B p_y^A p_y^B|$ , which corresponds to combinations of atomic excited states or non-Hund states.<sup>30</sup> Ionic configurations have rather smaller contributions (CI weight  $\leq 0.03$  in the singlet). The next-lying excited state above the septet shown in Table 1 is at least 2 eV higher in energy.

Judgement from the weights in the CASCI expansion would suggest that only the 20 unpaired neutral configurations could be used in the wave function expansion for all spin eigenstates. However, this approximation results in a flat spin ladder, with the same energy for all states. As described in the Introduction Section, neutral configurations are not able to account for the effective antiferromagnetic interactions between the open shells. The ladder is flat because MOs are strictly localized so that the direct exchange ( $K_{ab}$ ) ferromagnetic contribution is very small, actually null in the precision used. The first reasonable level of approximation, named neu + single ion in Table 1, is an expansion containing 20 neutral configurations plus all the 60 symmetry-allowed “metal-to-metal” (or nitrogen-to-nitrogen) ionic single excitations that can be constructed from the set of neutral configurations, e.g.,  $|p_z^B p_z^A p_x^B p_x^A p_y^B p_y^A|$ . The energy values obtained with this expansion are within 0.001 eV of the CASCI reference, and the number of configurations used is five-fold smaller. Since localized MOs are used, excitations between MOs that belong to the same irrep of  $C_{\infty v}$  are symmetry allowed. A second approximation can be made by including neutral and single ionic excitations only between localized MOs composed by the same atomic functions (neu +  $p_x, p_y, p_z$  ion, Table 1). This results in identical energies showing that symmetry-allowed “crossed” ionic excitations (e.g.,  $p_x^B \rightarrow p_y^A$ ) do not interact with the wave function for the low-lying states of neutral  $N_2$ . An expansion including neutral and the 12 single ionic excitations between the  $2p_z$  MOs (neu +  $p_z$  ion) results in energies within 0.01 eV of the CASCI reference. This suggests a third level of approximation in which the only ionic excitations included are those between MOs composed of atomic functions with large overlap (the  $z$  axis is the intermolecular axis). As a counter example, an expansion including neutral and ionic excitations between MOs composed of atomic functions with small overlap (neu +  $p_x, p_y$  ion) results in almost no antiferromagnetic contributions and a spin ladder in large disagreement with the CASCI reference. It should be noted that, by progressively removing from the CI space the excitations between  $2p_x$  and  $2p_y$  MOs (as in neu +  $p_x, p_y, p_z$  ion and in neu +  $p_z$  ion), spin ladders of higher energy and different space symmetry will not be correctly described. This is not a problem for neutral  $N_2$  because the next-lying state above the  $^7\Sigma$  state is much higher in energy, but it might

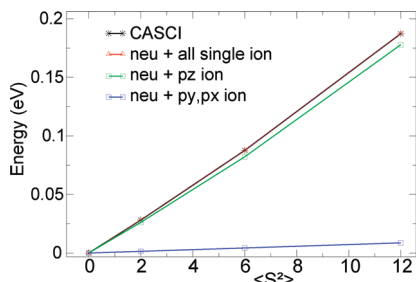


**Figure 1.** Spin ladders for the lowest energy total spin eigenstates of  $N_2^0$  calculated with different wave function expansions. See text for details.

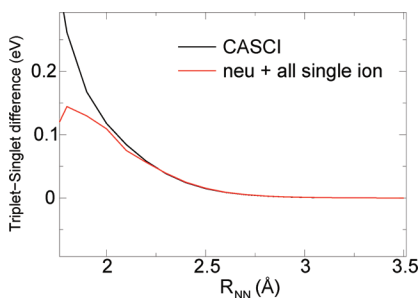


**Figure 2.** Triplet-singlet energy gap for varying  $N_2^0$  bond distances.

introduce errors when the ground spin ladder is near degenerate to other ladders.

Double ionic ( $N^{2-}-N^{2+}$ ), triple ionic ( $N^{3-}-N^{3+}$ ), and internal paired neutral configurations, e.g.  $|p_z^A p_z^B p_x^A p_x^B\rangle$ , which also corresponds to non-Hund atomic states, have very small contributions and can be safely neglected. Removing the two neutral configurations corresponding to the  $^4S$  high-spin state on each N atom from the expansion neu + single ion or using only these two neutral configurations plus all single ionic ones results in an incomplete spin manifold and, consequently, bogus spin ladders.

Linear spin ladders, i.e., ladders that follow a regular Landé splitting, are obtained within the CASCI, and the levels of approximation suggested above are shown in Figure 1. The CASCI ladder and the expansion named neu + single ion have both correlation coefficients to a straight line of 0.9994 and a F variance quality of 1662. The expansion neu +  $p_z$  ion has a correlation of 0.9992 and a F variance quality of 1187. In conclusion, the CI expansion neu + single ion captures the essential physics of exchange interactions for the ground spin ladder (Table 1) as well as for higher energy ladders (not shown) of the stretched dinitrogen molecule.

To test the limits of the proposed configuration selection, the singlet-triplet energy gap was calculated with varying bond distances. Figure 2 shows that the expansion neu + single ion results in energy gaps in very good agreement with the CASCI wave function down to bond distances of  $\sim 2.0$  Å. Below this distance, the interaction between the unpaired electrons is strong, and covalent bonding becomes appreciable. The system is not only spin coupled, and the proposed approximate CI selections do not apply.

**3.2.  $N_2^{2+}$ .** For  $N_2^{2+}$ , the configuration obtained after localizing the high-spin ROHF MOs is equivalent to the neutral  $N_2$  configuration (see above) but with two previous

highest occupied molecular orbitals (HOMOs) now unoccupied. The relative energies obtained for the lowest energy spin eigenstates are shown in Table 1. The expansion neu + single ion results in energy values in excellent agreement (within 0.002 eV) with the CASCI reference. For less than half-filled open shells, there are ionic configurations which still have all electrons unpaired. There are 36 of such unpaired ionic configurations for  $N_2^{2+}$ . An expansion including all neutral configurations, unpaired ionic and single ionic excitations between the  $2p_z$  MOs (neu + unpair,  $p_z$  ion) result in energies identical to the neu + single ion expansion. Single ionic excitations between MOs composed by atomic functions with small overlap (e.g.,  $p_y^B \rightarrow p_y^A$ ) and crossed single excitations do not interact with the wave function for the low-lying states of  $N_2^{2+}$ . A selection of the neutral configurations included in the expansions is possible for the open-shell systems without exactly half-full shells, i.e., more or less than half-filled and mixed valence. An expansion including only neutral configurations with one electron in each  $2p_z$  MOs, unpaired ionic and single ionic excitations between the  $2p_z$  MOs (neu  $p_z$  + unpair,  $p_z$  ion) also result in energies identical to the neu + single ion expansion. An expansion including all neutral configurations and the 24 single ionic excitations between the  $2p_z$  MOs (neu +  $p_z$  ion) results in energies within 0.01 eV of the CASCI reference. But, contrary to the equivalent neu +  $p_z$  ion expansion for the neutral  $N_2$ , an excess antiferromagnetic character is observed. This is a consequence of neglecting the ferromagnetic contribution of unpaired ionic configurations, easily seen in the results for the neu + unpair ion expansion in Table 1. Thus, not all metal-to-metal ionic excitations give an antiferromagnetic contribution to spin coupling, but only those that alter the number of unpaired electrons.

Considering a particle-hole symmetry, an equivalent behavior would be observed for the more than half-filled case. For example, in  $N_2^{2-}$ , ionic configurations without an empty MO give ferromagnetic contributions, equivalent to the ionic unpaired configurations in the less than half-filled case.

**3.3.  $N_2^-$ .** For  $N_2^-$ , the localized high-spin ROHF MOs used in the CI expansions were obtained for the neutral dinitrogen to avoid an artificial polarization of the occupied MOs and thereof biased CI results. Similar results were obtained if a fractional occupation of the MOs was allowed in the ROHF solution. The relative energies obtained for the lowest energy spin eigenstates are shown in Table 1. Delocalization of the excess electron stabilizes the “neutral” configurations resulting in a ferromagnetic CASCI spin ladder. This is the double-exchange effect.<sup>11</sup> Antiferromagnetic contributions by the superexchange mechanism are an order of magnitude smaller. Thus, an expansion including only neutral configurations (neu, Table 1) accounts for the double-exchange effect and results in energies within 0.02 eV of the CASCI reference. In fact, an expansion (neu  $p_z$ ) in which the excess electron occupies only the  $2p_z$  orbitals has identical results. However, by removing from the CI space configurations in which the excess electron occupies the  $2p_x$  and  $2p_y$  MOs, spin ladders

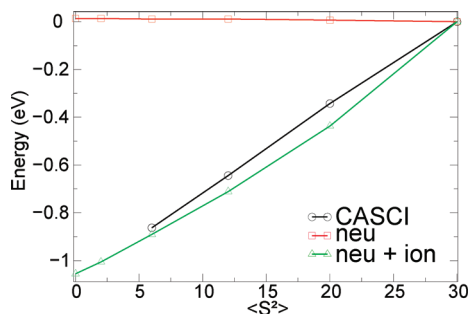


**Figure 3.** Spin ladders for the lowest energy total spin eigenstates of  $\text{Cr}_2$  at 4.4 bohr separation calculated with different wave function expansions.

with higher energy and different space symmetry will not be correctly described, as observed for similar CI selections in  $\text{N}_2^{0/+2}$ .

The antiferromagnetic contribution can be retrieved in an expansion including all symmetry-allowed single ionic excitations (neu + single ion) resulting in energies within 0.0001 eV of the CASCI reference. The expansion including the interacting neutral and the 24 single ionic excitations between the  $2p_z$  MOs (neu  $p_z + p_z$  ion) contains five-fold less configurations than the CASCI and results in energies within 0.001 eV of this reference.

**3.4.  $\text{Cr}_2$ .** For the stretched dichromium molecule, covalent bonding between the 3d orbitals is not significant. However, there is still a  $\sigma$  bond formed mostly between the diffuse 4s chromium orbitals.<sup>31</sup> The correct energy ordering for the total spin states should have the antiferromagnetic singlet as the ground state and the ferromagnetic undecaplet as the highest energy state of the ground spin ladder.

The canonical high-spin ROHF solution has 10 singly occupied MOs formed by antisymmetric and symmetric combinations of the atomic 3d functions. The HOMO-1 and HOMO are formed, respectively, by antisymmetric and symmetric combinations of the 4s functions. After full orbital localization, each Cr atom contains six electrons and a configuration corresponding to a  $^7\text{S}$  atomic state. The active space was composed of the 12 electrons in 10 MOs formed by 3d functions and the 2 MOs formed by 4s functions. All the configurations used in the expansions were formed out of the two possible combinations of the localized 4s orbitals consistent with a  $\sigma$  bonding MO. The CASCI solution was only computed down to the quintet state. The secular determinants necessary to obtain states with  $S < 2$  were too large and could not be built due to memory limitations (see Computational Methods Section).

Figure 3 shows spin ladders calculated for  $\text{Cr}_2$  under different CI selections. The undecaplet state was chosen as zero of energy. An expansion including only unpaired neutral configurations (252 configurations in total), e.g.,  $[\text{core}]d_z^A d_z^B d_x^A d_x^B d_y^A d_y^B d_{x^2-y^2}^A d_{x^2-y^2}^B d_{xy}^A d_{xy}^B d_{xz}^A d_{xz}^B d_{yz}^A d_{yz}^B$ , yields an incorrect spin ladder with a high-spin ground state, as expected from the direct-exchange contribution to spin coupling. The expansion neu + single ion, including all 252 unpaired neutral configurations plus 1260 ionic configurations, results in fair agreement with the CASCI result (within 0.1 eV). Ionic configurations were built from the set of unpaired

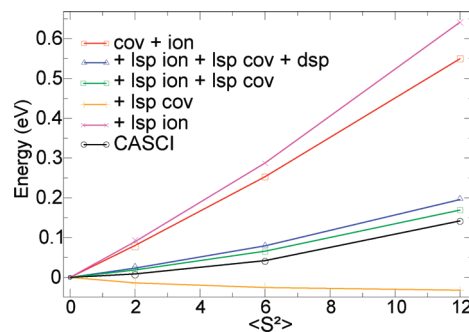


**Figure 4.** Spin ladders for the lowest energy total spin eigenstates of  $\text{NFN}^-$  in angular geometry calculated with different wave function expansions.

neutral configurations by metal-to-metal single excitations between MOs belonging to the same irreps of the  $C_{\infty v}$  group. It should be noted that the neu + single ion CI expansion contains only 1512 configurations, instead of the 63 504 configurations that would be necessary to expand the singlet state in the CASCI wave function. Energies within 0.01 eV of the neu + single ion expansion are obtained by a smaller expansion with 952 configurations that does not contain the crossed ionic excitations between MOs belonging to the same  $C_{\infty v}$  irrep but formed by different atomic functions, e.g.,  $d_{xz}^A \rightarrow d_{yz}^B$ .

The spin ladders obtained with CASCI and neu + single ion approximation have, respectively, correlation coefficients to a straight line of 0.9998 and 0.996 and a F variance quality of 4032 and 465. The approximations proposed for the model stretched dinitrogen are equally valid for the stretched dichromium and result in a reduction of at least two orders of magnitude in the size of the CI space.

**3.5.  $\text{NFN}^-$  in  $C_{2v}$  Symmetry.** On the following sections, the proposed approximations are tested on compounds containing diamagnetic bridges. Localized MOs were obtained for angular  $\text{NFN}^-$  from a high-spin ROHF solution. Each nitrogen has a double-occupied 2s-like shell and 3 unpaired electrons in orbitals composed by the 2p functions. Fluoride has 4 double-occupied orbitals composed by 2s and 2p functions. All 9 MOs formed by p functions and 12 electrons are included in the active space.

Figure 4 shows spin ladders calculated under different CI selections. The singlet was chosen as zero of energy. An expansion including only unpaired neutral and ionic single excitations between the magnetic (nitrogen) centers with the bridge (fluoride) MOs left double occupied (neu + single ion, 80 configurations in total) yields a largely antiferromagnetic ladder, in large disagreement with the CASCI reference. The ligand spin polarization has to be included for a qualitatively correct description of the  $\text{NFN}^-$  wave function.

LSP configurations are obtained by LMCT *single* excitations built from the set of neutral and ionic determinants. An expansion including the neu + single ion set and all configurations generated from the (20) neutral determinants by LMCT single excitations (+ lsp neu, 280 configurations in total) results in an overestimation of the ferromagnetic interactions. On the other hand, a similar expansion (+ lsp ion, 406 configurations in total) but with LSP configurations

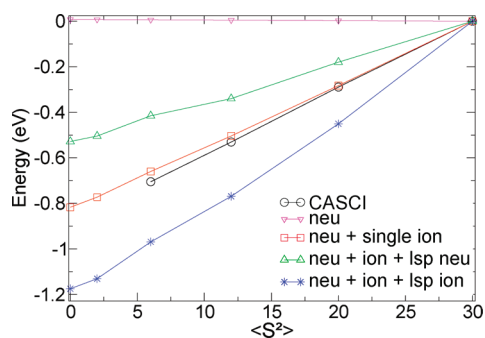


**Figure 5.** Spin ladders for the lowest energy total spin eigenstates of linear  $\text{Fe}_2\text{S}^{4+}$  calculated with different wave function expansions.

generated by single excitation from the (60) ionic determinants results in an overestimation of the antiferromagnetic contributions. A proper balance is obtained by an expansion including the neu + single ion set plus both neutral and ionic ligand spin polarization (+ lsp ion + lsp neu), resulting in energies within 0.03 eV of the CASCI reference. Double LMCT excitations can also be constructed from the neutral and ionic configurations set by either exciting the same bridge orbital or two different ones. The resulting contributions are anti- and ferromagnetic but with much smaller magnitude ( $\sim 0.01$  eV), as found for other TM bridged systems.<sup>8,7</sup>

In other words, the set of unpaired neutral and single ionic configurations might be considered a zero-order reference set. LSP excitations built out of this multireference set result in anti- and ferromagnetic contributions to spin coupling if the excitation originates from an ionic or a neutral configuration, respectively. For  $\text{NFN}^-$ , the LSP contributions are larger than the through-space superexchange contributions and have to be included for a qualitatively correct description of the spin coupling. This is not generally true, as shown below for the TM compounds. DSP contributions are relatively small and can be removed from the CI space without affecting the results significantly.

**3.6. Linear  $\text{Fe}_2\text{S}^{4+}$ .** Localized MOs were obtained for linear  $\text{Fe}_2\text{S}^{4+}$  from a high-spin ROHF solution. Each metal center has a half-filled valence shell with 5 unpaired electrons in 5 orbitals composed by 3d functions, corresponding to an atomic  $^6\text{S}$  state. The sulfur bridge has four double-occupied 2s- and 2p-like orbitals. The 3 outer-valence bridge MOs and the 10 MOs formed by iron 3d functions were included in the active space, with the respective 16 electrons.

A CASCI solution with such a large active space is not feasible within the memory limitations found here (see Computational Methods Section). Instead, Figure 5 shows a CASCI result obtained with only 10 electrons in the 10 MOs formed by iron 3d functions. The undecaplet state was chosen as zero of energy. The neu expansion includes only unpaired neutral configurations with double-occupied ligand MOs (252 configurations in total, Figure 5) and results in small ferromagnetic coupling, as observed above for the chromium dimer. The neu + single ion expansion includes the ionic configurations (1512 configurations in total) and results in very good agreement with the 10 electron in 10 orbitals CASCI. The effect of neutral LSP configurations (neu + ion + lsp neu) is ferromagnetic, and the ionic LSP (neu + ion

**Table 2.** Relative Energies (eV) for  $\text{Fe}_2\text{S}_2^{2+}$  Lowest Energy Spin Eigenstates Calculated with Two Different CI Expansions

$\langle \hat{S}^2 \rangle$	neu + single ion	CASSCF
0	0.000	0.000
2	0.041	0.046
6	0.135	0.136
12	0.283	0.267
20	0.475	0.427
30	0.717	0.679

+ lsp ion) is antiferromagnetic. Neutral and ionic LSP configurations are obtained by LMCT *single* excitations built from the set of neutral (neu) and ionic (ion) determinants, respectively. However, contrary to the  $\text{NFN}^-$  example above, through-space superexchange dominates, and the ligand spin polarization is relatively smaller in  $\text{Fe}_2\text{S}^{4+}$ . For example, the ladder obtained with the expansion neu + ion + lsp neu is antiferromagnetic. In fact, inclusion of both neutral and ionic LSP configurations practically cancels out the polarization effect and results in a spin ladder very close to the neu + single ion expansion. Even if LMCT excitations are not explicitly included in the CI space, the effect of bridges and ligands is at least partially included when MOs are generated and when energies of the zero-order multireference configurations are calculated. Results similar to those shown in Figure 5 for the neu + single ion expansion are obtained by removing the crossed ionic excitations, as observed above for stretched  $\text{N}_2$  and  $\text{Cr}_2$ , leading an expansion with only 952 configurations.

**3.7.  $\text{Fe}_2\text{S}_2^{2+}$  Ring.** The final example is the iron–sulfur cluster  $\text{Fe}_2\text{S}_2^{2+}$ . Localized MOs obtained from a high-spin ROHF solution show a half-filled valence 3d shell with 5 unpaired electrons in each iron center. Each sulfur bridge has 3 outer-valence double-occupied localized MOs composed by 2p functions. An active space containing all 16 valence MOs and the respective 22 electrons is only feasible using modern direct CI procedures. An ab initio CASSCF computation using such large active space is taken as reference in Table 2. The CASSCF singlet wave function is expanded in almost two million determinants in comparison to the approximate and much shorter expansion neu + single ion that includes only 1512 determinants corresponding to the unpaired neutral and ionic single excited states. The agreement between the CASSCF and the selected neu + single ion expansion is very good (within 0.05 eV) and suggests that this level of approximation captures the essential physics of spin coupling in transition-metal complexes. In fact, energies within 0.003 eV of the neu + single ion expansion were obtained with an even smaller expansion containing 952 configurations, by removing the crossed ionic excitations.

## 4. Conclusions

Approximate configuration interaction expansions were introduced for the calculation of wave functions with correct spin and space symmetries of weakly coupled transition-metal compounds with many open shells. The selection of configurations included in the CI space was based on physical

arguments for the mechanisms of spin coupling, namely direct exchange, superexchange, double exchange, and ligand spin polarization. In the spirit of valence-bond calculations, localized (molecular) orbitals were used in the construction of Slater determinants. But, instead of specifying a level of excitation as in the normal CI terminology, the expansions included all determinants needed to complete the spin manifold compatible with the exchange mechanisms depicted in the Introduction Section.

A zero-order multireference set was identified as the set of neutral and single ionic configurations. The neutral set accounts for the direct-exchange ferromagnetic mechanism and corresponds to configurations with an equivalent number of unpaired electrons in each magnetic site (excluding the excess electron in mixed valence systems). The ionic set is built by symmetry-allowed metal-to-metal single excitations from the neutral set that alter the total number of unpaired electrons. For all the spin-coupled compounds tested here and, we believe, for any spin-coupled system, single ionic excitations are enough to account for the through-space superexchange antiferromagnetic mechanism.

Symmetry-allowed excitations involve molecular orbitals that belong to the same irrep of the *localized* MOs point group. The contribution of symmetry-allowed crossed ionic excitations, i.e., excitations between MOs formed mainly by different atomic functions, was very small or null for the ground spin ladder in all molecules studied. For other systems, this result will depend on the localization method employed and on whether the localized MOs resemble pure atomic orbitals or combinations thereof. Even smaller expansions are possible by selectively removing from the CI space other ionic configurations or neutral configurations for the more or less than half-filled and mixed valence systems that have very small or null CI weights in the expansions of the low-lying spin states. For instance, removing excitations between MOs formed by atomic functions with a small overlap in N<sub>2</sub> resulted in energies close to those obtained with the full zero-order set for the ground spin ladder. However, spin ladders of higher energy and different space symmetry might not be correctly described by CI spaces smaller than the zero-order multireference set.

Ligand-to-metal charge-transfer configurations constructed from the zero-order reference set account for ligand spin polarization and double spin polarization. Single LMCT out of the neutral set always give a ferromagnetic contribution. On the other hand, single LMCT out of the ionic set always give an antiferromagnetic contribution, sometimes called “through-bond” superexchange. The LSP configurations should be included in the CI space whenever this contribution is comparable in magnitude to through-space direct and superexchange. For the iron–sulfur compounds studied here, the LSP contribution is small and approximately cancels out when both ionic and neutral single LMCT excitations are included. This is not a general result,<sup>9,10,30</sup> but it is a valuable one in reducing the size of the CI expansions. A related argument is valid for the mixed valence system tested. The double-exchange effect in N<sub>2</sub><sup>-</sup> is much larger

than the superexchange so that ionic configurations can be excluded from the CI space without affecting the energy splittings significantly.

Comparisons with experimental *J* coupling constants are not given here. Such comparisons would not be fair at this stage because the calculations presented do not include the effect of dynamic correlation, which is essential for quantitative results.<sup>27,9</sup> Dynamic correlation can be added on top of the zero-order set by either multireference CI or perturbative corrections.<sup>27</sup> If a semiempirical method is employed, then correlation can be implicitly included in the parametrization of electron-repulsion integrals.

The proposed approximations result in much shorter CI expansions. For example, the CASSCF result obtained with  $2 \times 10^6$  configurations for Fe<sub>2</sub>S<sub>2</sub><sup>2+</sup> is reproduced with about 10<sup>3</sup> configurations. However, the exponential scaling of the CI space size is not entirely ameliorated. Polynuclear compounds with a larger number of magnetic centers and unpaired electrons will still require large configurational spaces that may exceed the available computational resources even if including only neutral and single ionic excitations between neighboring sites. Nevertheless, identifying the spin-coupling mechanisms with valence-bond structures and including controlled approximations in the CI expansion may open the way to treat these more challenging systems.

**Acknowledgment.** Jeppe Olsen (University of Århus) is acknowledged for helpful discussions. G.M.A. acknowledges funding from FAPESP, projects 07/52772-6 and 07/59345-6.

**Supporting Information Available:** Semiempirical parameters and the procedure used for their calibration. This material is available free of charge via the Internet at <http://pubs.acs.org>.

## References

- (1) Blondin, G.; Girerd, J.-J. *Chem. Rev.* **1990**, *90*, 1359–1376.
- (2) Heisenberg, W. *Z. Phys.* **1928**, *49*, 619–636.
- (3) Dirac, P. *Proc. R. Soc. London, Ser. A* **1929**, *123*, 714–733.
- (4) Anderson, P. W. *Phys. Rev.* **1950**, *79*, 350–356.
- (5) Anderson, P. W. *Phys. Rev.* **1959**, *115*, 2–13.
- (6) Hay, P. J.; Thibault, J. C.; Hoffmann, R. *J. Am. Chem. Soc.* **1975**, *97*, 4884–4899.
- (7) de Loth, P.; Cassoux, P.; Daudey, J. P.; Malrieu, J. P. *J. Am. Chem. Soc.* **1981**, *103*, 4007–4016.
- (8) Noodleman, L.; Davidson, E. R. *Chem. Phys.* **1986**, *109*, 131–143.
- (9) Calzado, C. J.; Cabrero, J.; Malrieu, J. P.; Caballol, R. *J. Chem. Phys.* **2002**, *116*, 2728–2747.
- (10) Calzado, C. J.; Angeli, C.; Taratiel, D.; Caballol, R.; Malrieu, J.-P. *J. Chem. Phys.* **2009**, *131*, 044327.
- (11) Zener, C. *Phys. Rev.* **1951**, *82*, 403–405.
- (12) Noodleman, L.; Han, W.-G. *J. Biol. Inorg. Chem.* **2006**, *11*, 674–694.
- (13) Noodleman, L. *J. Chem. Phys.* **1981**, *74*, 5737–5743.

- (14) Soda, T.; Kitagawa, Y.; Onishi, T.; Takano, Y.; Shigeta, Y.; Nagao, H.; Yoshioka, Y.; Yamaguchi, K. *Chem. Phys. Lett.* **2000**, *319*, 223–230.
- (15) Sinnecker, S.; Neese, F.; Noodleman, L.; Lubitz, W. *J. Am. Chem. Soc.* **2004**, *126*, 2613–2622.
- (16) Li, J.; Noodleman, L. In *Spectroscopic Methods in Bioinorganic Chemistry*; Solomon, E. I., Hodgson, K. O., Eds.; ACS Symposium Series: Washington, DC, 1998; Vol. 692.
- (17) Nair, N. N.; Schreiner, E.; Pollet, R.; Staemmler, V.; Marx, D. *J. Chem. Theory Comput.* **2008**, *4*, 1174–1188.
- (18) Cabrero, J.; Amor, N. B.; de Graaf, C.; Illas, F.; Caballol, R. *J. Phys. Chem. A* **2000**, *104*, 9983–9989.
- (19) Hubner, O.; Sauer, J. *J. Chem. Phys.* **2002**, *116*, 617–628.
- (20) Dewar, M. J.; Thiel, W. *J. Am. Chem. Soc.* **1977**, *99*, 4899–4907.
- (21) Thiel, W. Semiempirical Methods. In *Modern Methods and Algorithms of Quantum Chemistry*; Grotendorst, J., Ed.; John von Neumann Institute for Computing: Jülich, Germany, 2001; Vol. 3, pp 1–24.
- (22) Stewart, J. J. P. *J. Comput.-Aided Mol. Des.* **1990**, *4*, 1–45.
- (23) Stewart, J. J. P. *MOPAC 2000*; Fujitsu Limited, Tokyo, Japan, 1999.
- (24) Dewar, M. J.; Zoebisch, E. G.; Healy, H. F.; Stewart, J. P. P. *J. Am. Chem. Soc.* **1985**, *107*, 3902–3909.
- (25) Thiel, W.; Voityuk, A. A. *J. Phys. Chem.* **1996**, *100*, 616–626.
- (26) Pipek, J.; Mezey, P. *J. Chem. Phys.* **1989**, *90*, 4916–4926.
- (27) Helgaker, T.; Jørgensen, P.; Olsen, J. *Molecular Electronic-Structure Theory*, 1st ed.; Wiley: New York, 2000; pp 523–645.
- (28) Karlstrom, G.; Lindh, R.; Malmqvist, P.-Å.; Roos, B. O.; Ryde, U.; Veryazov, V.; Widmark, P.-O.; Cossi, M.; Schimmelpfennig, B.; Neogrady, P.; Seijo, L. *Comput. Mater. Sci.* **2003**, *28*, 222.
- (29) Roos, B. O.; Lindh, R.; Malmqvist, P.-A.; Veryazov, V.; Widmark, P.-O. *J. Phys. Chem. A* **2005**, *109*, 6575–6579.
- (30) Bastardis, R.; Guihéry, N.; de Graaf, C. *J. Chem. Phys.* **2008**, *129*, 104102.
- (31) Goodgame, M. M.; Goddard, W. A., III *Phys. Rev. Lett.* **1985**, *54*, 661–664.

CT1001279